

# UC Irvine

## UC Irvine Previously Published Works

### Title

Eco-Driving Algorithm with a Moving Bottleneck on a Single-Lane Road

### Permalink

<https://escholarship.org/uc/item/6762n8cc>

### Authors

Sun, Pengyuan  
Yang, Dingtong  
Jin, Wen-Long

### Publication Date

2020-12-01

### DOI

10.1177/0361198120961381


### Copyright Information

This work is made available under the terms of a Creative Commons Attribution License, available at <https://creativecommons.org/licenses/by/4.0/>

Peer reviewed

# Eco-Driving Algorithm with a Moving Bottleneck on a Single-Lane Road

Pengyuan Sun<sup>1</sup>, Dingtong Yang<sup>1</sup>, and Wen-Long Jin<sup>1</sup>

Transportation Research Record  
2020, Vol. 2674(12) 493–504  
© National Academy of Sciences:  
Transportation Research Board 2020  
Article reuse guidelines:  
sagepub.com/journals-permissions  
DOI: 10.1177/0361198120961381  
journals.sagepub.com/home/trr  


## Abstract

Eco-driving strategies have been applied to smooth traffic flow and reduce greenhouse gas emissions along with air pollution. In this paper, we propose an eco-driving strategy to reduce traffic oscillation and smooth trajectories for connected vehicles following a moving bottleneck on a single-lane road. The eco-driving strategy, which leverages vehicle-to-vehicle (V2V) communications, designs advisory speed limits for each following vehicle through a control algorithm. The algorithm is based on the prediction of the following vehicle trajectories dictated by a moving bottleneck. The following vehicle trajectories are obtained by analytically solving the moving bottleneck problem in which the moving bottleneck speeds vary over time. In addition, the bounded acceleration rate is imposed in car-following behavior. The benefits of this strategy are demonstrated by applying it to four scenarios with different bottleneck movements. By simulating the scenarios with Newell's car-following model with bounded acceleration and VT-Micro emission model, we find that both speed fluctuations and emissions are reduced with the algorithm in the scenarios in which the moving bottleneck has a constant speed, accelerates, decelerates and stops-and-goes. The results indicate that the proposed eco-driving algorithm can smooth traffic flow behind a moving bottleneck.

Greenhouse gas emissions contribute significantly to global warming and climate change (1). According to a recent study, 30% of energy consumption in the U.S. comes from the transportation sector, which is responsible for a significant portion of greenhouse gas emissions as well as air pollution (2). Fluctuations in traffic flow lead to frequent accelerations and decelerations, which can cause additional greenhouse gas emissions and air pollution, and worsen environmental conditions (3).

Eco-driving refers to a set of driving modes and strategies which reduce greenhouse gas emissions and air pollution. Eco-driving can be achieved through multiple control mechanisms. Traffic oscillation smoothing is a conventional approach to achieve eco-driving (4). Setting an advisory speed limit is one method for reducing traffic oscillation by adjusting the speed limits for individual vehicles. Instead of instantly controlling the speed of a vehicle, setting an advisory speed limit provides a relatively consistent control output, which allows vehicles to adjust their speeds according to the real-time traffic. Setting an advisory speed limit has the benefit of addressing safety issues and is easily executable (5, 6).

Recently, connected vehicle (CV) technologies have enabled real-time vehicle-to-vehicle (V2V) and vehicle-to-infrastructure (V2I) communications, which have been applied to provide advisory speed limits to smooth

vehicle trajectories. Examples of these CV integrated eco-driving strategies include setting advisory speed limits for vehicles approaching traffic signals; passing through work zones; and traveling along the highways (7–10). Taking advantage of V2V communications among connected vehicles, this paper introduces a new eco-driving strategy based on advisory speed limits for vehicles following a moving bottleneck. This strategy is applicable to a situation in which a moving bottleneck is presented on an uncongested single-lane road, and the bounded acceleration rate is imposed on car-following behaviors. A moving bottleneck is caused by a slow-moving vehicle with a speed lower than that of the mainstream traffic (11). A bounded acceleration rate refers to the maximum acceleration that the vehicle could reach. In this study, we assume that the initial traffic flow is with the free-flow speed, and we consider the situations that the moving bottleneck could travel with either constant speed or varying speeds. The advisory speed limits for the

<sup>1</sup>Department of Civil and Environmental Engineering, Institute of Transportation Studies, 4060 Anteater Instruction and Research Building (AIRB), University of California, Irvine, CA

**Corresponding Author:**  
Pengyuan Sun, pengyuas@uci.edu

following vehicles are designed based on the following trajectories. The following vehicle trajectories are obtained by solving the moving bottleneck problem analytically.

The moving bottleneck problem derives the traffic flow impeded by the bottleneck. Existing literature provides various methods with which to solve the problem by following the first moving bottleneck model and by considering the problem as an extension of the Lighthill–Whitham–Richards (LWR) model (11–14). Daganzo and Laval solved the problem by using numerical methods (15, 16). Later, Leclercq and Jin and Laval implement the bounded acceleration rate into the moving bottleneck problem (17, 18). In previous studies, the moving bottleneck problem mainly deals with fixed and (or) constant moving bottlenecks. This paper extends the literature in moving bottleneck studies by solving the problem with a varying speed bottleneck. In this part, we use Newell's car-following model with bounded acceleration to describe the vehicle movements (19). We also utilize the LWR model with bounded acceleration to derive the traffic states upstream of the moving bottleneck and the trajectories of the following vehicles (18, 20, 21). Based on the vehicle trajectories and V2V communications, we develop an algorithm to design advisory speed limits for the following vehicles, with the objectives of reducing traffic oscillation and emissions. We also test the algorithm with numerical examples of different bottleneck movements and use the VT-Micro model to calculate vehicle emissions (4). We compare the vehicle emissions and the average speed of the following vehicles to show the benefit of using the algorithm. From the simulation results, the eco-driving strategy can achieve an emission reduction and maintain a smoother traffic flow, and at the same time, the algorithm does not decrease the average speeds of the following vehicles.

The contributions of this study are as follows. First, we further extend the literature on the moving bottleneck problem to a more general case, in which the moving bottleneck travels with varying speeds. We solve the general moving bottleneck problem analytically and derive trajectories of the vehicles following the moving bottleneck. In addition, we propose a new eco-driving algorithm by setting advisory speed limits based on the following vehicles' trajectories. Finally, we use numerical examples to demonstrate that this strategy could smooth traffic flow and reduce emissions under different bottleneck movements, maintaining the same average speeds as the scenarios without applying the algorithm.

The reminder of this paper is organized as follows. The next section provides the notation for variables and parameters used throughout this paper. Then, we present the analytical results of the moving bottleneck problem on a single-lane road. The following section presents the

control algorithm we proposed to achieve the eco-driving. The numerical examples are demonstrated in the penultimate section. The final section draws conclusions from this paper and proposes further studies.

## Notation

We use the notation listed in Table 1 throughout the paper.

## Moving Bottleneck Problem on a Single-Lane Road

### Constant Speed Moving Bottleneck Problem with Bounded Acceleration

A bottleneck on a road could be a slow-moving vehicle occupying a road lane, and the behaviors of the following vehicles are significantly impacted by the leading bottleneck (12, 16). We apply the LWR model to derive the traffic flow density upstream of the moving bottleneck at each location and each time. The well-known LWR model is derived by differentiating the cumulative flow for the time and location and can be written as Equation 1 (20, 21).

$$\frac{\partial k(x, t)}{\partial t} + \frac{\partial Q(k(x, t))}{\partial x} = 0 \quad (1)$$

We assume that vehicles have a bounded acceleration rate and tend to move as fast as possible. Let  $A$  be the bounded acceleration rate, the LWR model with bounded acceleration can be implemented as Equation 2, in which  $\varepsilon$  is an infinitesimal number (18, 22). This function shows that if vehicles have to accelerate, they travel as fast as they can; but all vehicles cannot accelerate beyond the bound acceleration rate  $A$ .

$$\frac{\partial v(x, t)}{\partial t} + \frac{\partial v(x, t)}{\partial x} \cdot v(x, t) = \min\left\{\frac{V(k) - v}{\varepsilon}, A\right\} \quad (2)$$

A fundamental diagram shows the relationship between the flow rate and density. In this study, we apply a triangular fundamental diagram which is shown in Equation 3.

$$Q(k) = \min\{uk, w(k_j - k)\} \quad (3)$$

Combining the LWR model and the triangular fundamental diagram, we assume all the vehicles obey Newell's car-following model with bounded acceleration. We apply Equation 4a and b to update the following vehicle velocities and positions respectively at each time step.

$$V(t + \Delta t, n) = \min\left\{u, \frac{X(t, n-1) - X(t, n) - \rho}{\tau}, V(t, n) + A \cdot \Delta t\right\} \quad (4a)$$

**Table 1.** Notation of Variables and Parameters

Notation	Description
<b>Basic traffic flow parameters</b>	
$k(x, t)$	Traffic density at location $x$ and time $t$
$q(x, t)$	Traffic flow rate at location $x$ and time $t$
$v(x, t)$	Vehicle speed at location $x$ and time $t$
$A$	Bounded acceleration rate
$\mu$	Free-flow speed
$w$	Shock wave speed in congested traffic
$k_j$	Jam density in the fundamental diagram
$\tau$	Time gap between two adjacent vehicles
$\rho$	Jam spacing in the fundamental diagram
<b>Moving bottleneck problem</b>	
$k_1$	Initial traffic density
$q_1$	Initial traffic flow rate
$k_b$	Traffic density at the bottleneck location
$q_b$	Traffic flow rate at the bottleneck location
$v_b(t)$	Bottleneck speed at time $t$
$v_s(t)$	Shock wave speed at time $t$
$b(t)$	Trajectory of the moving bottleneck
$m(t)$	Shock wave curve in the upstream traffic flow after the moving bottleneck
<b>Eco-driving algorithm</b>	
$\psi(t)$	Estimated leading vehicle trajectory as the moving bottleneck
$\phi_n(t)$	Original trajectory of the vehicle $n$ according to the leading vehicle
$\tilde{\phi}_n(t)$	Redesigned trajectory of the following vehicle $n$
$v_n^{ASL}$	Advisory speed limit for the following vehicle $n$
$t_n^*$	Vehicle $n$ end time for applying advisory speed limit
$t_0$	Time when the leading vehicle becomes a moving bottleneck
$x_n^0$	Location of vehicle $n$ when the leading vehicle arrives

$$X(t + \Delta t, n) = \min\{X(t, n) + u \cdot \Delta t, X(t, n) + \Delta t \cdot \frac{X(t, n-1) - X(t, n) - \rho}{\tau}, X(t, n) + \Delta t \cdot V(t, n) + A \cdot \Delta t^2\} \quad (4b)$$

For a single-lane road, the properties of shock waves and rarefaction waves could be derived through the LWR model and the fundamental diagram (11, 21). In the previously published literature, Jin and Laval and Leclercq analytically solve the constant moving bottleneck problem with bounded acceleration (18, 23). If the moving bottleneck enters a road with a lower speed, it creates a traffic state behind it, which is different from the initial uncongested state. A shock wave is generated at the boundary of the two traffic states. If the bottleneck moves at a constant speed, the shock wave also propagates at a constant speed. The speed of the shock waves ( $v_s$ ) is derived by Equation 5. After the moving bottleneck leaves, rarefaction waves are generated as following vehicles accelerate at each time until the following traffic flow speed reaches the free-flow speed. The shock waves and rarefaction waves between different traffic states are collectively called characteristic waves.

$$v_s = \frac{q_1 - q_b}{k_1 - k_b} \quad (5)$$

If a triangular fundamental diagram is applied (Equation 3), we can write the density and flow rate of the affected traffic as Equation 6.

$$\begin{cases} q_b = k_b v_b \\ q_b = -w(k_b - k_j) \end{cases} \quad (6)$$

The results for a constantly moving bottleneck problem with bounded acceleration are shown in Figure 1. This result represents the case in which the upstream is uncongested.

The speeds for shock waves and rarefaction waves can be derived from the fundamental diagram shown in Figure 1a, and the following vehicle trajectories are shown in Figure 1b.

### Generalized (Varying Speed) Moving Bottleneck Problem with Bounded Acceleration

In previous studies, bottlenecks have been treated as either stationary or as moving at a constant speed, which are special cases in reality (12, 18, 23). However, in generalized situations, the bottleneck usually travels with varying speeds. The situation could occur if the moving bottleneck is traveling through a curve, meeting a ramp-way, or impacted by varying wind resistance. As a result,

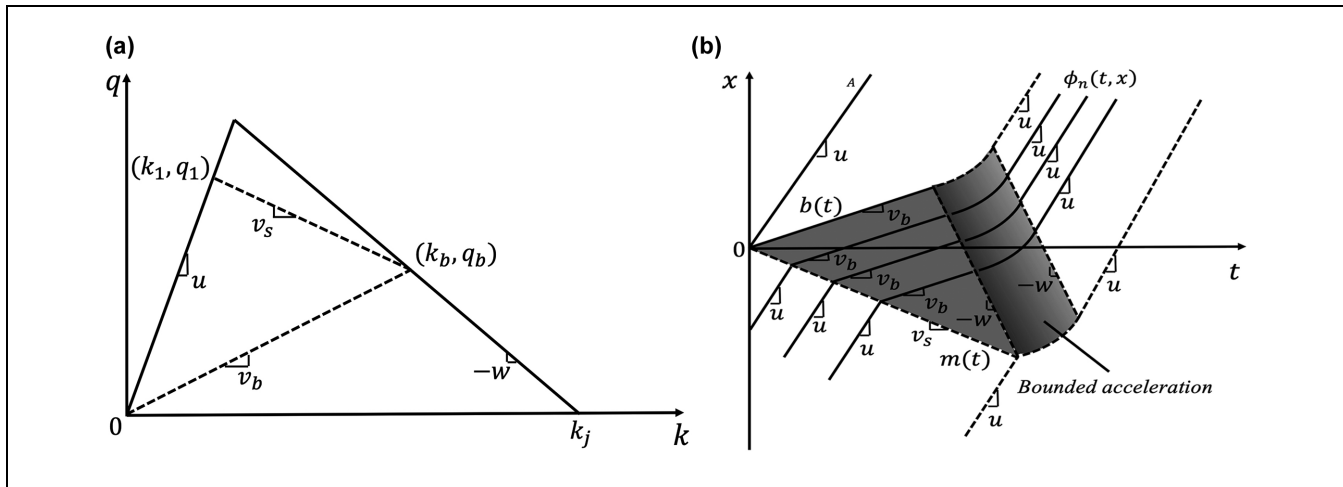


Figure 1. Analytical solution for the moving bottleneck with constant speed: (a) fundamental diagram, and (b) vehicle trajectories.

the conclusions and results from a constantly moving bottleneck are no longer applicable in these situations. In this subsection, we derive the trajectories of the following vehicles by solving a generalized (varying speed) moving bottleneck problem with bounded acceleration.

If a varying speed moving bottleneck enters the road segment with a speed lower than the free-flow speed, it begins to create traffic states which are different from the initial uncongested state. As long as the bottleneck is in the road section, it keeps creating traffic states when its speed changes. As the bottleneck moving speed is less than the free-flow speed, these traffic states are all at lower speeds than the uncongested state. Once a new traffic state is created, characteristic waves are generated between the new traffic state and others. At every time step, these characteristic waves propagate until they merge into other waves. The traffic behind the bottleneck is alternating between different states, as the speed of the bottleneck changes.

Figure 2a shows different traffic states and waves in the fundamental diagram. The initial upstream traffic state is at  $(k_1, q_1)$ . The moving bottleneck speed is  $v_b(t)$ , which varies over time. If the moving bottleneck enters the road at  $t = 0$  with the speed of  $v_b(0)$  ( $v_b(0) < u$ ) between the initial state  $(k_1, q_1)$  and the first congested traffic state  $(k_b(0), q_b(0))$ , a shock wave forms with the initial propagation speed of  $v_s(0)$ . As the bottleneck speeds are varying, congested traffic states are created along the congestion curve (with the slope of  $-w$ ) of the triangular fundamental diagram.

Figure 2b shows the corresponding traffic states and characteristic waves of Figure 2a in  $x - t$  space. At  $t = 0$ , the bottleneck enters the road with an initial speed  $v_b(0)$  ( $v_b(0) < u$ ), and a shock wave and the initial propagation speed  $v_s(0)$  is generated. The speed can be derived from Equation 5 and the triangular fundamental diagram. As

the bottleneck speed  $(v_b(t))$  changes with time, characteristic waves are generated and propagated until they merge into the shock wave curve  $(m(t))$ . The instantaneous speed of the shock wave at each time is derived from the traffic state generated along with the characteristic wave, and the upstream initial state. In Figure 2, a and b, and the formulations below,  $t_1$  is the time point when one characteristic wave is generated from the bottleneck;  $t$  is the time point when this wave merges into the shock wave.  $q_1$  and  $k_1$  are the flow rate and density of the upstream flow.

$$\frac{dm(t)}{dt} = v_s(t) \tag{7}$$

$$\frac{db(t)}{dt} = v_b(t) \tag{8}$$

Equations 7 and 8 describe the relationship between speed and trajectory in  $x - t$  space. For both the bottleneck trajectory  $(b(t))$  and the shock wave curve  $(m(t))$ , the speeds at each time, that is,  $v_b(t)$  and  $v_s(t)$  respectively, are derived from taking the derivatives.

$$\frac{m(t) - b(t_1)}{t - t_1} = -w \tag{9}$$

$$v_s(t) = v_b(t_1) \tag{10}$$

$$v_s(t) = \frac{q_1 - q_b(t_1)}{k_1 - k_b(t_1)} \tag{11}$$

Equations 9–11 demonstrate the features of shock waves and rarefaction waves. In Equation 9, the characteristic wave is generated from the bottleneck at time  $t = t_1$  and propagates backward with the speed of  $w$ . When the characteristic wave meets and merges to the shock wave  $(m(t))$ , at the time  $t$ , the speed of the shock wave is derived from Equations 10 and 11.

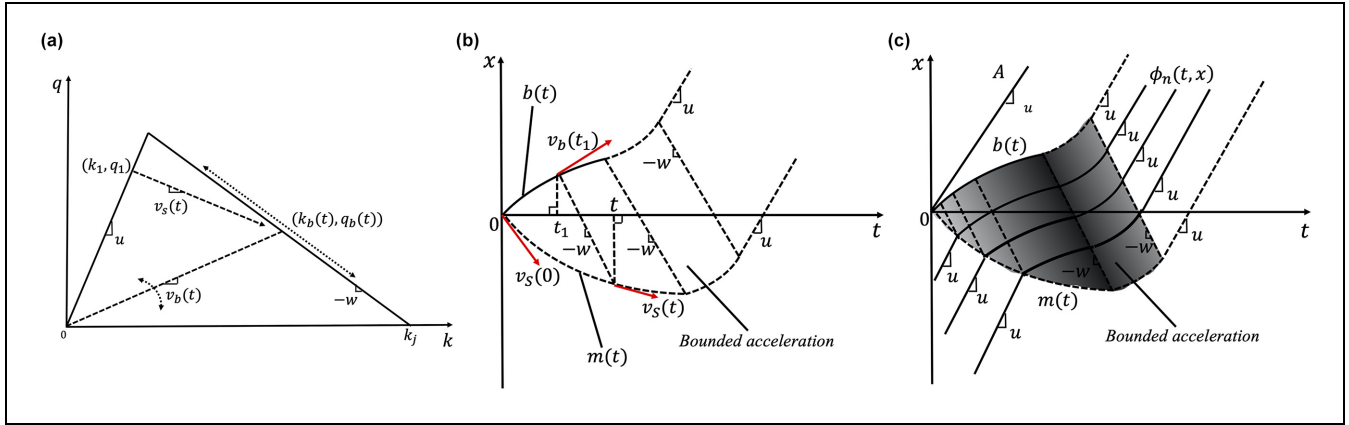


**Figure 2.** Analytical solution for the moving bottleneck with varying speeds: (a) fundamental diagram, (b) characteristic waves, and (c) vehicle trajectories.

$$q_b(t_1) = k_b(t_1)v_b(t_1) \tag{12}$$

$$q = Q(k) \tag{13}$$

Equation 12 is the constitutive law to derive the traffic condition including the density and flow rate at the time  $t = t_1$ , when the bottleneck is with the varying speeds of  $v_b(t_1)$ . To derive  $k_b(t_1)$  and  $q_b(t_1)$ , the relationship between the flow rate and density is needed and is shown in the fundamental diagram Equation 13.

If the triangular fundamental diagram Equation 3 is applied, we can derive the traffic state at each time caused by the moving bottleneck from Equation 14, where  $k_b(t_1)$  and  $q_b(t_1)$  are the density and flow rate at the bottleneck location at the time  $t = t_1$ .

$$\begin{cases} k_b(t_1) = \frac{1}{\tau \left( \frac{d(b(t))}{dt} \right)_{t_1} + \tau w} \\ q_b(t_1) = \frac{\left( \frac{d(b(t))}{dt} \right)_{t_1}}{\tau \left( \frac{d(b(t))}{dt} \right)_{t_1} + \tau w} \end{cases} \tag{14}$$

Finally, based on the traffic states caused by the moving bottleneck at each time  $(k_b(t), q_b(t))$ , and the initial traffic state  $(k_1, q_1)$ , the shock wave curve  $(m(t))$  could be generalized into the form of a first-order linear differential equation, which is shown in Equation 15. If the moving bottleneck trajectory  $(b(t))$  is given, combined with Equations 14 and 15, the shock wave curve could be analytically derived by solving the differential equation.

$$\begin{cases} \frac{dm(t)}{dt} = \frac{q_1 - q_b(t_1)}{k_1 - k_b(t_1)} \\ \frac{m(t) - b(t_1)}{t - t_1} = -w \end{cases} \tag{15}$$

At the same time, the moving bottleneck problem analysis could also derive the trajectories of the following vehicles, through the densities and flow rates of traffic states at each time and location. For example, if all the vehicles

obey Newell’s car-following model with bounded acceleration, and the bottleneck is decelerating and then leaves the road, the following trajectories are shown in Figure 2c. If the following vehicles are being impeded by the moving bottleneck, the following trajectories repeat the moving bottleneck trajectory after entering the shock wave curve. When the bottleneck disappears, if the following vehicle speeds are lower than the free-flow speed, the following vehicles will accelerate at the bounded acceleration rate until they reach the free-flow speed. The following vehicle trajectories, which are derived from solving the moving bottleneck problem, are the foundation of deriving the eco-driving strategy in the next section.

## Eco-Driving Strategy

### Overview of the Control Algorithm

In the previous section, we derived the vehicle trajectories impeded by the moving bottleneck. The moving bottleneck leads to additional traffic oscillation, and empirically, traffic oscillation leads to extra gas emissions. Considering the factors above, we propose a control algorithm as the eco-driving strategy, to reduce the level of gas emissions. The objective of reducing gas emissions is achieved by reducing the speed oscillation. This algorithm applies to connected vehicles and operates on a single-lane road, in which the traffic flow is uncongested (with the free-flow speed) before being affected by the moving bottleneck. Such traffic situations could occur if a CV merges into an uncongested road with a speed less than the free-flow speed or if a CV begins to decelerate and then leaves the road. Different from conducting trajectory design, the proposed control algorithm in this study provides the control output as a static advisory speed limit. The advisory speed limit for

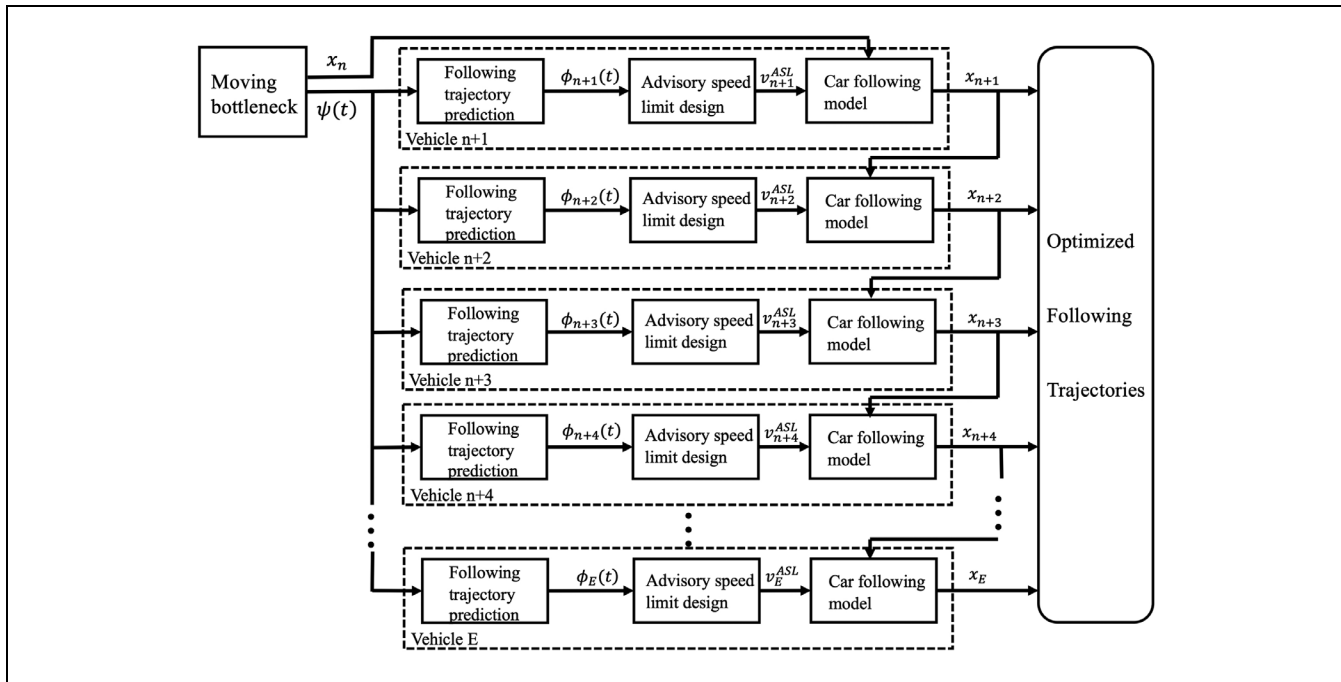


**Figure 3.** Control system of the eco-driving algorithm.

each individual following vehicle is generated through a control framework as shown in Figure 3. In this section, we define the CV which impedes the initial uncongested traffic flow, that is, the moving bottleneck, as the leading vehicle; other vehicles being affected by the leading vehicle are the following vehicles. The control objective is to reduce traffic oscillation and emissions by setting advisory speed limits for the following vehicles. We assume the leading CV has a planned leading trajectory and will follow the trajectory for the road segment. Delays in communication and computation processes are omittable. Under these assumptions, we can obtain an upper bound performance by applying the algorithm.

Figure 3 demonstrates the eco-driving control algorithm, and this algorithm is operated through the following steps.

*Step 1.* Broadcasting the leading vehicle (moving bottleneck)'s trajectory

The leading vehicle shares the estimated trajectory to the following vehicles if it begins to impede the upstream traffic flow on the road. It follows the planned movement trajectory ( $\tilde{x} = \psi(t)$ ) until it leaves the road or reaches the free-flow speed.

*Step 2.* Predicting the following vehicles' trajectories

Based on the leading vehicle trajectory ( $\psi(t)$ ), the following vehicles predict their original following trajectories

( $\tilde{x} = \phi_n(t)$ ) by using the analytical results from the generalized varying speed moving bottleneck problem.

*Step 3.* Calculating the advisory speed limit and the control duration

The advisory speed limit for each following vehicle (i.e.,  $v_n^{ASL}$  for the following vehicle  $n$ ) is decided by taking the tangent line of the following trajectory from Step 2. The duration for applying the speed limit (i.e.,  $t_n^*$  for the following vehicle  $n$ ) can also be derived from the point of tangency which is further elaborated in the advisory speed limit and control duration section.

*Step 4.* Executing the advisory speed limits

Each following vehicle adjusts its advisory speed limit during the execution duration (i.e., from  $t = t_0$  to  $t = t_n^*$  for the following vehicle  $n$ ). After that, each following vehicle speed limit is changed back to the free flow speed respectively.

### Advisory Speed Limit and the Control Duration

The control outputs include the static advisory speed limit ( $v_n^{ASL}$ ) and the ending algorithm time ( $t_n^*$ ) for each following vehicle. In optimization jargon, the objective is to minimize the level of emissions for various harmful gas, which is shown in Equation 16, in which  $f(\cdot)$

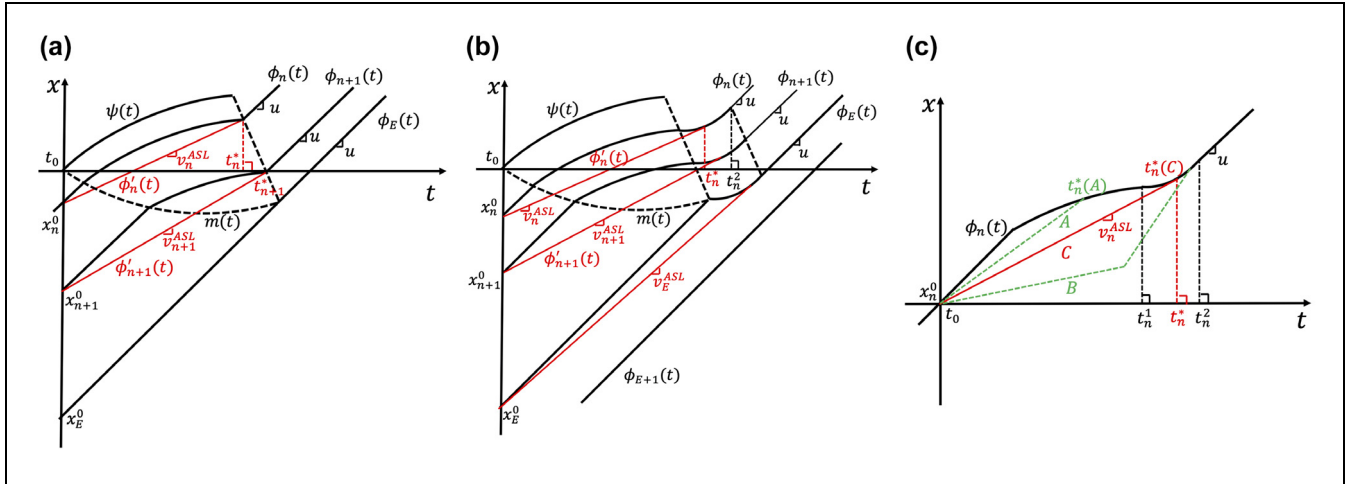


**Figure 4.** Advisory speed limit and control duration: (a) unbounded acceleration, (b) bounded acceleration, and (c) advisory speed limit design.

calculates the emissions for a given vector of the advisory speed limits  $\overrightarrow{v}^{ASL}$ .

$$\min E = f\left(\overrightarrow{v}^{ASL}\right) \quad (16)$$

However, owing to the complexity of the objective function (non-convex), the optimal solution is hard to obtain. In addition, the objective functions are based on different gas emissions and various emission models, which include parameters with uncertainty. As a result, the optimal solution may not be accurate and universal for different circumstances. Considering the factors above, we apply the speed oscillation function as the control objective for each following vehicle (Equation 17), in which  $t_0$  and  $t_n^2$  are the time points when the moving bottleneck occurs and when the following vehicle regains the free-flow speed respectively;  $a_n(t)$  is the following vehicle acceleration at each time between  $[t_0, t_n^2]$ .

$$\min \sigma = \int_{t_0}^{t_n^2} (a_n(t))^2 dt \quad (17)$$

The constraints for setting the static advisory speed limit are shown in Equations 18–21, in which  $\phi'_n(t)$  denotes the redesigned trajectory of the following vehicle  $n$  after applying the advisory speed limit  $(v_n^{ASL})$ .

$$\begin{cases} \phi'_n(t) - \psi(t) \geq \rho + \tau \frac{d(\phi'_n(t))}{dt} & (n = 1) \\ \phi'_n(t) - \phi'_{n-1}(t) \geq \rho + \tau \frac{d(\phi'_n(t))}{dt} & (n > 1) \end{cases} \quad (\forall t \in [t_0, t_n^2]) \quad (18)$$

$$\frac{d^2(\phi'_n(t))}{dt^2} \leq A \quad (\forall n, \forall t \in [t_0, t_n^2]) \quad (19)$$

$$\frac{d(\phi'_n(t))}{dt} = v_n^{ASL} \quad (\forall n, \forall t \in [t_0, t_n^*]) \quad (20)$$

$$\phi'_n(t_n^2) = \phi_n(t_n^2) \quad \forall n \quad (21)$$

Among the constraints shown above, Equation 18 ensures that each following vehicle travels safely after applying the advisory speed limit, with the actual time gap no less than the time gap ( $\tau$ ) in Newell’s car-following model. Equation 19 ensures that the acceleration cannot exceed the bounded acceleration rate  $A$  anywhere along the redesigned trajectory  $(\phi'_n(t))$ . Equation 20 sets the advisory speed limit assuming that the redesigned trajectory  $(\phi'_n(t))$  is static during the algorithm control duration  $([t_0, t_n^*])$ . Equation 21 ensures that the original following trajectory  $(\phi_n(t))$  and the redesigned trajectory  $(\phi'_n(t))$  meet at the same location when the vehicle regains the free-flow speed at  $t = t_n^2$ . As a result, Equation 21 ensures that the algorithm does not change the vehicle average speed during the impediment period  $([t_0, t_n^2])$ .

In this study, a heuristic solution is considered for setting the advisory speed limit. The design of the advisory speed limit and control duration is shown in Figure 4. Obviously, the objective  $\sigma$  in Equation 17 is non-negative and equals zero when the vehicle travels at a constant speed. When the vehicle applies the static advisory speed limit  $(v_n^{ASL})$  during the algorithm application period  $[t_0, t_n^*]$ , Equation 17 is equivalent to the surrogate objective function in Equation 22, that is, the advisory speed



limit algorithm is executed for the longest possible duration in the impediment period  $[t_0, t_n^*]$ .

$$\max t_n^* (t_n^* \in [t_0, t_n^2], \forall n) \quad (22)$$

Figure 4a analyzes the case in which the bounded acceleration rate is not considered (excluding Equation 19 from the constraints). The minimum possible value of the objective function (Equation 17, minimize the speed fluctuation) is zero when the vehicle keeps a stable speed. To satisfy the constraint of Equation 21, the vehicle needs to travel at a speed that equals the average speed without the control algorithm. Therefore, the average speed is set to be the advisory speed limit ( $v_n^{\text{ASL}}$ ) for vehicle  $n$ , and the new trajectory  $\phi_n'(t)$  is derived. As  $\phi_n'(t)$  shares the same starting/ending points as those of the original trajectory ( $\phi_n(t)$ ), and  $\phi_n'(t) \leq \phi_n(t)$ , the redesigned trajectory satisfies the safety constraint and causes no further time to be lost, that is, the redesigned trajectory keeps the same average speed during the impediment.

Figure 4b shows the trajectory redesign after introducing the bounded acceleration constraint (Equation 19). As the following vehicle speeds are inevitably affected by the leading vehicle ( $v_b(t) < u$ ), the following vehicles will experience an acceleration period ( $[t_n^1, t_n^2]$ ) to resume the free-flow speed. In this case, the advisory speed limit is set as the slope of the tangent line from the origin trajectory at  $t = t_0$ . The tangent point in the acceleration period should be the end time point for applying the advisory speed limit ( $t = t_n^*$ ). From the solution of the moving bottleneck problem, during the acceleration period, the original following trajectory ( $\phi_n(t)$ ) is with the bounded acceleration, that is,  $\frac{d^2(\phi_n(t))}{dt^2} = A$ . As the redesigned trajectory ( $\phi_n'(t)$ ) merges into the original following trajectory ( $\phi_n(t)$ ) at the tangent point in the acceleration period,  $\phi_n'(t)$  also satisfies the constraint in Equation 19.

Figure 4c demonstrates that the redesigned trajectory will also maximize the surrogate objective function (Equation 22) if the advisory speed limit ( $v_n^{\text{ASL}}$ ) is designed as the tangent line of the original trajectory, (i.e.,  $\max t_n^* = t_n^*(C)$ ). If the advisory speed limit for vehicle  $n$  is set to be greater than the tangent line slope (e.g., Trajectory C is the tangent line, and the advisory speed limit associated with Trajectory A is greater than tangent slope), the vehicle could potentially experience another deceleration as well as a longer acceleration period ( $t_n^*(A) < t_n^*(C)$ ). Therefore, the speed oscillation is not minimized. On the other hand, if the advisory speed limit for vehicle  $n$  is smaller than the tangent slope (e.g., Trajectory B), unavoidably, the vehicle would either encounter a further decrease in the vehicle average travel speed (violating the constraint in Equation 21); or need to adjust the advisory speed limit more than once (no longer a static advisory speed limit, violating the

**Table 2.** Settings of the Simulation

Parameters	Values
$u$ , Free flow speed	20 m/s (45 mph)
$n$ , Following vehicle number	20
$A$ , Bounded acceleration rate	2 m/s <sup>2</sup> (6.56 ft/s <sup>2</sup> )
$\Delta t$ , Simulation time step	1 s

constraint in Equation 20). Therefore, Trajectory B is not feasible. In contrast, Trajectory C could achieve both operational simplicity and trajectory smoothness without a further decrease in the average speed of the following vehicle. Therefore, the advisory speed limit should be set to be the slope of the tangent line (Trajectory C).

$$\begin{cases} v_n^{\text{ASL}} = \frac{\phi_n(t_n^*) - x_n^0}{t_n^* - t_0} \\ \left( \frac{d\phi_n(t)}{dt} \right)_{t_n^*} = v_n^{\text{ASL}} \end{cases} \quad t_n^* \in [t_n^1, t_n^2] \quad (23)$$

According to Figure 4c, the advisory speed limit ( $v_n^{\text{ASL}}$ ) and the algorithm ending time ( $t_n^*$ ) for the vehicle  $n$  are derived together from Equation 23. The vehicle  $n$  travels with the advisory speed limit from  $(t_0, x_n^0)$ , and its redesigned trajectory tangents to the original trajectory at the algorithm ending point  $(t_n^*, \phi_n(t_n^*))$ .

## Numerical Examples of Connected Vehicles on an Arterial Section

In this section, the effectiveness of the eco-driving strategy is tested in four numerical traffic scenarios. The leading vehicle has different movements, namely, traveling at a constant speed (lower than the free-flow speed), accelerating, decelerating, and executing a stop-and-go for pick-up or drop-off. In each scenario, trajectories of following vehicles with and without applying this eco-driving algorithm are compared.

In the simulation, a CV platoon is initially travelling at the free-flow speed on a straight single-lane road. The road length is sufficient for all vehicles to apply the algorithm. Newell's car-following model with bounded acceleration is applied to update the vehicle speed and location at every time step. The total simulation time is 300 s, and the moving bottleneck occurs at  $t = 100$ s when the traffic is at an uncongested steady state. The parameter settings for the simulations are shown in Table 2.

We compare the trajectories with and without the advisory speed limit from  $t_0$  to  $t_n^*$  (Figure 4c) for all following vehicles in all scenarios. Each simulation includes one leading vehicle and 20 following vehicles.

To understand the potential environmental benefits of applying the eco-driving strategy, we calculate the three

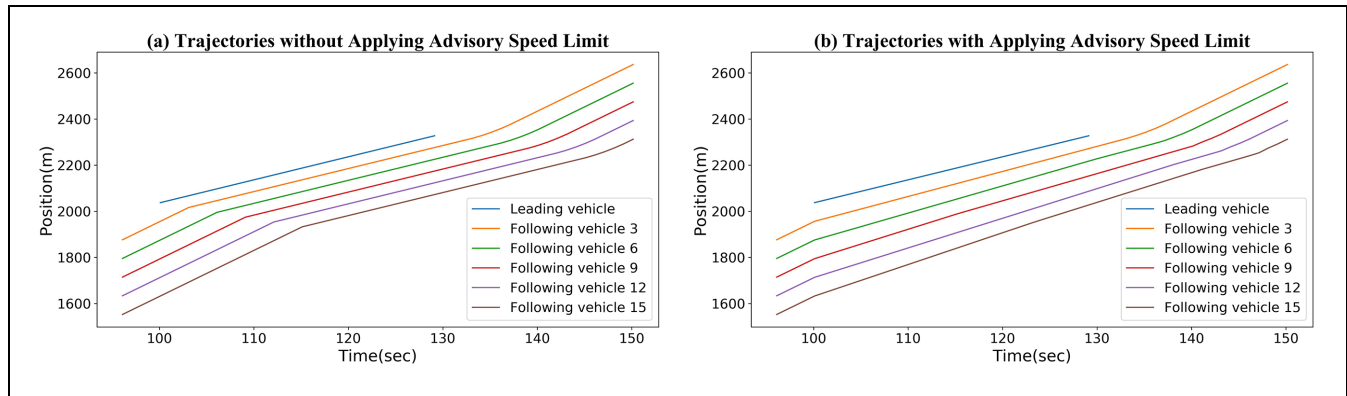


**Figure 5.** A comparison of vehicle trajectories (a) without and (b) with application of the eco-driving strategy with a constant speed moving bottleneck.

kinds of gas emissions in each traffic scenario. There are several models to estimate the gas emissions for vehicles, such as the Comprehensive Modal Emission Model (CMEM), and the SUMO pollutant emission models (24, 25). In this study, we use the VT-Micro model because of its simplicity and accuracy (4). Equation 24 shows the regression models of each emission rate, which are estimated by a combination of linear, quadratic, and cubic terms of real-time speeds and accelerations.

$$\ln(moe_e(t)) = \begin{cases} \sum_{i=0}^3 \sum_{j=0}^3 L_{ij}^e v^j(t) a^i(t) & a(t) \geq 0 \\ \sum_{i=0}^3 \sum_{j=0}^3 M_{ij}^e v^j(t) a^i(t) & a(t) < 0 \end{cases} \quad (24)$$

in which  $moe_e(t)$  is the emission rate for the type of gas ( $e$ ),  $v(t)$  and  $a(t)$  are the instantaneous speed and acceleration rate at time  $t$ , and  $M_{ij}^e$  and  $L_{ij}^e$  are the acceleration and deceleration coefficients respectively for the VT-Micro regression model of each kind of gas. For emissions, this study uses the hydrocarbon (HC), carbon monoxide (CO), and carbon dioxide (CO<sub>2</sub>) emissions as measurements of the gas emissions. We assume that all vehicles in the simulation are identical, and with the same mechanical performance and emission standard.

We use the speed standard deviation of all the following vehicles to evaluate the traffic oscillation reduction. To make the comparisons clear without losing generality, we plotted five of the 20 following vehicles for comparison in the following figures.

### Constant Moving Bottleneck

We first run the simulation with a constant speed moving bottleneck. The moving bottleneck occurs at  $t = 100$ s with a speed of 10m/s (22mph). The leading vehicle stays at the road section for 30s and leaves. Figure 5, a and b, show the trajectories of the vehicles without and

with application of the eco-driving strategy respectively. For both of the two subfigures, the blue line represents the trajectory of the bottleneck, the other lines represent the trajectories of the following vehicles. From the simulation results, the trajectories with the eco-driving control algorithm are smoother than those without the algorithm.

To further analyze the algorithm performance in vehicle speed oscillation smoothing, we calculated the standard deviation of speed. By applying this eco-driving strategy, the average speed standard deviation decreased by 64.3% by comparing the same scenario with and without the algorithm. As a result, the overall traffic oscillation has been significantly reduced. The algorithm could also reduce different gas emissions. In addition, we calculated the average speeds of all the following vehicles during leading vehicle impacted periods, and the result shows the algorithm does not generate an additional decrease in the following vehicle speed, which has no effect on traffic mobility. The statistical results for the constantly moving bottleneck scenario are listed in Table 3.

### Accelerating and Decelerating Bottlenecks

In the second and third scenarios, we test the eco-driving strategy performances in which the moving bottleneck is accelerating or decelerating, respectively.

For the acceleration scenario, we set the leading vehicle's initial speed to be 10m/s (22mph). The leading vehicle accelerates with a constant acceleration of 1 m/s<sup>2</sup> (3.28 ft/s<sup>2</sup>) until it reaches the free-flow speed. After that, as the leading vehicle maintains the free-flow speed afterward and has no impediment for the upstream traffic, the vehicle is not a moving bottleneck anymore. For the decelerating case, we assume that the bottleneck is decelerating at a rate of 1 m/s<sup>2</sup> for 10s from the free-flow speed, and it leaves the road after 10s. Tables 4 and 5 list

**Table 3.** Statistics of Speed and Gas Emissions with and without Applying the Eco-Driving Strategy with a Constant Speed Moving Bottleneck

	Non eco-driving	Eco-driving	Difference
Average speed (m/s) (mph)	12.64 (28.27)	12.64 (28.27)	0.0%
Speed standard deviation	4.46	1.59	-64.3%
HC (mg)	439.13	383.67	-12.6%
CO <sub>2</sub> (g)	558.8	573.2	-2.5%
CO (g)	16.60	15.94	-4%

Note: mph = miles per hour; HC = hydrocarbon; CO = carbon monoxide; CO<sub>2</sub> = carbon dioxide.

**Table 4.** Statistics of Speed and Gas Emissions with and without Applying the Eco-Driving Strategy with an Accelerating Moving Bottleneck

	Non eco-driving	Eco-driving	Difference
Average speed (m/s) (mph)	17.50 (39.14)	17.50 (39.14)	0.0%
Speed standard deviation	3.37	1.17	-65.3%
HC (mg)	223.9	140.9	-37.1%
CO <sub>2</sub> (g)	333.5	291.5	-12.5%
CO (g)	10.74	8.99	-16.3%

Note: mph = miles per hour; HC = hydrocarbon; CO = carbon monoxide; CO<sub>2</sub> = carbon dioxide.

**Table 5.** Statistics of Speed and Gas Emissions with and without Applying the Eco-Driving Strategy with a Decelerating Moving Bottleneck

	Non eco-driving	Eco-driving	Difference
Average speed (m/s) (mph)	17.26 (38.61)	17.26 (38.61)	0.0%
Speed standard deviation	3.24	0.983	-69.7%
HC (mg)	300.3	255.7	-14.9%
CO <sub>2</sub> (g)	406.6	363.6	-10.6%
CO (g)	12.82	11.03	-14.0%

Note: mph = miles per hour; HC = hydrocarbon; CO = carbon monoxide; CO<sub>2</sub> = carbon dioxide.

the average speed, speed standard deviation, and gas emissions with and without applying this strategy in the two cases. From these results, when the leading vehicle accelerates and decelerates, this algorithm does not change the average speed and it reduces traffic oscillation and gas emissions.

### Stop-and-Go Scenario

In the last scenario, we simulated the leading vehicle travelling with a more complicated movement, that is, a stop-and-go. The leading vehicle begins to decelerate at  $t = 100$ s. The deceleration rate is  $-2 \text{ m/s}^2$  ( $-6.56 \text{ ft/s}^2$ ). Then, the vehicle stops for 5 s, at the location  $x = 2100$ m. At  $t = 115$ s, this vehicle begins to accelerate with the acceleration rate of  $2 \text{ m/s}^2$  and reaches the free-flow speed after 10 s. This situation occurs if a vehicle needs

to pick up a passenger for example. Figure 6 shows the trajectories with and without applying this eco-driving strategy, and the emissions and speed statistical results are listed in Table 6. As the result shows, after applying the algorithm, the following traffic flow is smoother, as the following vehicles do not experience long decelerating and accelerating periods.

### Conclusions and Future Work

In this paper, we extended the existing research on the moving bottleneck problem, formulated the moving bottleneck problem if the bottleneck travels with varying speeds and solved the problem analytically. Based on the following vehicle trajectories derived from the moving bottleneck problem, we proposed an eco-driving algorithm that enforces an advisory speed limit to reduce the

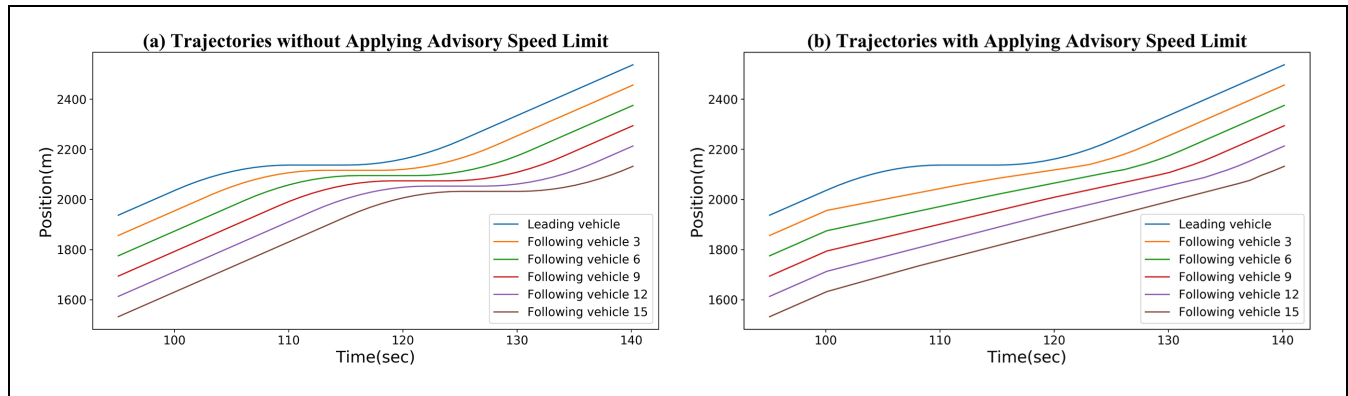


**Figure 6.** A comparison of vehicle trajectories (a) without and (b) with application of the eco-driving strategy with the ‘stop and go’ bottleneck.

**Table 6.** Statistics of Speed and Gas Emissions with and without Applying the Eco-Driving Strategy with a ‘Stop and Go’ Bottleneck

	Non eco-driving	Eco-driving	Difference
Average speed (m/s) (mph)	11.06 (24.74)	11.06 (24.74)	0.0%
Speed standard deviation	8.17	2.34	-71.4%
HC (mg)	399.37	348.94	-12.6%
CO <sub>2</sub> (g)	459.0	412.9	-10.0%
CO (g)	13.39	11.90	-11.2%

Note: mph = miles per hour; HC = hydrocarbon; CO = carbon monoxide; CO<sub>2</sub> = carbon dioxide.

traffic oscillation and emissions. We further tested the effectiveness of the eco-driving algorithm using a set of simulations. We compared the standard deviation of speeds and the different types of emissions. According to the simulation results, the standard deviation of the vehicle speed decreases up to 71.4% after applying the algorithm, and gas emission was reduced by 10%–40%. The results indicate that the eco-driving algorithm is capable of smoothing traffic and reducing emissions. It is also worth noting that the proposed algorithm does not change the average speeds for the vehicles if they are following the moving bottleneck.

Several further studies could be extended from this study. This study focuses on the moving bottleneck case on a single-lane road. For a road section with multiple lanes, this eco-driving strategy may also have similar effects on smoothing trajectories and reducing emissions. We are also interested in applying this algorithm with different moving bottleneck movements and different car-following behaviors. In addition, this study assumes the following vehicles are all connected, and we will consider using this algorithm if the following vehicles are partly connected in the future, and we are interested in what the effect will be in that scenario. In addition, this algorithm can be extended into dynamic real-time speed

control algorithms with specific objective functions, although this paper focuses more on analytical analysis and a heuristic vehicle trajectory redesign. As the leading vehicle movement estimation and the communications between vehicles cannot be totally accurate and timely, other considerations should be included such as communication delays, leading vehicle estimation updating, and transmission ranges. Moreover, the basic idea of this study was to combine conventional traffic flow theories with advanced traffic technology. We believe it provides another theoretical basis to develop eco-driving strategies in the future.

### Acknowledgments

We would like to thank the associate editors and all anonymous reviewers for their help in improving this paper.

### Author Contributions

The authors confirm contribution to the paper as follows: study conception and design: Wen-Long Jin, Pengyuan Sun; data collection: Pengyuan Sun; analysis and interpretation of results: Wen-Long Jin, Pengyuan Sun, Dingtong Yang; draft manuscript preparation: Pengyuan Sun, Dingtong Yang. All authors reviewed the results and approved the final version of the manuscript.

### Declaration of Conflicting Interests

The author(s) declared no potential conflicts of interest with respect to the research, authorship, and/or publication of this article.

### Funding

The author(s) received no financial support for the research, authorship, and/or publication of this article.

### References

- Karl, T. R., J. M. Melillo, T. C. Peterson, and S. J. Hassol. (eds.). *Global Climate Change Impacts in the United States*. Cambridge University Press, New York, NY, 2009.
- Rakha, H. A., K. Ahn, K. Moran, B. Saerens, and E. Van den Bulck. Virginia Tech Comprehensive Power-Based Fuel Consumption Model: Model Development and Testing. *Transportation Research Part D: Transport and Environment*, Vol. 16, No. 7, 2011, pp. 492–503.
- Yang, H., and W. L. Jin. A Control Theoretic Formulation of Green Driving Strategies Based on Inter-Vehicle Communications. *Transportation Research Part C: Emerging Technologies*, Vol. 41, 2014, pp. 48–60.
- Ahn, K., H. Rakha, A. Trani, and Van M. Aerde. Estimating Vehicle Fuel Consumption and Emissions Based on Instantaneous Speed and Acceleration Levels. *Journal of Transportation Engineering*, Vol. 128, No. 2, 2002, pp. 182–190.
- Trayford, R. S., B. W. Doughty, and J. W. Van Der Touw. Fuel Economy Investigation of Dynamic Advisory Speeds from an Experiment in Arterial Traffic. *Transportation Research Part A: General*, Vol. 18, No. 5–6, 1984, pp. 415–419.
- Almqvist, S., C. Hydén, and R. Risser. Use of Speed Limiters in Cars for Increased Safety and a Better Environment. *Transportation Research Record: Journal of the Transportation Research Board*, 1991. 1318: 34–39.
- Ubierno, G. A., and W. L. Jin. Mobility and Environment Improvement of Signalized Networks through Vehicle-To-Infrastructure (V2I) Communications. *Transportation Research Part C: Emerging Technologies*, Vol. 68, 2016, pp. 70–82.
- Wan, N., A. Vahidi, and A. Luckow. Optimal Speed Advisory for Connected Vehicles in Arterial Roads and the Impact on Mixed Traffic. *Transportation Research Part C: Emerging Technologies*, Vol. 69, 2016, pp. 548–563.
- Kwon, E., D. Brannan, K. Shouman, C. Isackson, and B. Arseneau. Development and Field Evaluation of Variable Advisory Speed Limit System for Work Zones. *Transportation Research Record: Journal of the Transportation Research Board*, 2007. 2015: 12–18.
- Carsten, O. M., and F. N. Tate. Intelligent Speed Adaptation: Accident Savings and Cost-Benefit Analysis. *Accident Analysis & Prevention*, Vol. 37, No. 3, 2005, pp. 407–416.
- Gazis, D. C., and R. Herman. The Moving and “Phantom” Bottlenecks. *Transportation Science*, Vol. 26, No. 3, 1992, pp. 223–229.
- Newell, G. F. A Moving Bottleneck. *Transportation Research Part B: Methodological*, Vol. 32, No. 8, 1998, pp. 531–537.
- Leclercq, L., S. Chanut, and J. B. Lesort. Moving Bottlenecks in Lighthill-Whitham-Richards Model: A Unified Theory. *Transportation Research Record: Journal of the Transportation Research Board*, 2004. 1883: 3–13.
- Fadhoun, K., H. Rakha, and A. Loulizi. Analysis of Moving Bottlenecks Considering a Triangular Fundamental Diagram. *International Journal of Transportation Science and Technology*, Vol. 5, No. 3, 2016, pp. 186–199.
- Daganzo, C. F., and J. A. Laval. On the Numerical Treatment of Moving Bottlenecks. *Transportation Research Part B: Methodological*, Vol. 39, No. 1, 2005, pp. 31–46.
- Daganzo, C. F., and J. A. Laval. Moving Bottlenecks: A Numerical Method That Converges in Flows. *Transportation Research Part B: Methodological*, Vol. 39, No. 9, 2005, pp. 855–863.
- Leclercq, L. Bounded Acceleration Close to Fixed and Moving Bottlenecks. *Transportation Research Part B: Methodological*, Vol. 41, No. 3, 2007, pp. 309–319.
- Jin, W.-L., and J. Laval. Bounded Acceleration Traffic Flow Models: A Unified Approach. *Transportation Research Part B: Methodological*, Vol. 111, 2018, pp. 1–18.
- Newell, G. F. A Simplified Car-Following Theory: A Lower Order Model. *Transportation Research Part B: Methodological*, Vol. 36, No. 3, 2002, pp. 195–205.
- Lighthill, M. J., and G. B. Whitham. On Kinematic Waves II. A Theory of Traffic Flow on Long Crowded Roads. *Proceedings of the Royal Society of London, Series A: Mathematical and Physical Sciences*, Vol. 229, No. 1178, 1955, pp. 317–345.
- Richards, P. I. Shock Waves on the Highway. *Operations Research*, Vol. 4, No. 1, 1956, pp. 42–51.
- Jin, W. L. Nonstandard Second-Order Formulation of the LWR Model. *Transportmetrica B: Transport Dynamics*, Vol. 7, No. 1, 2019, pp. 1338–1355.
- Leclercq, L. Hybrid Approaches to the Solutions of the “Lighthill-Whitham-Richards” Model. *Transportation Research Part B: Methodological*, Vol. 41, No. 7, 2007, pp. 701–709.
- An, F., M. Barth, J. Norbeck, and M. Ross. Development of Comprehensive Modal Emissions Model: Operating under Hot-Stabilized Conditions. *Transportation Research Record: Journal of the Transportation Research Board*, 1997. 1587: 52–62.
- Krajzewicz, D., M. Behrisch, P. Wagner, R. Luz, and M. Krumnow. Second Generation of Pollutant Emission Models for SUMO. In *Modeling Mobility with Open Data* (Behrisch, M., and M. Weber, eds.), Springer, Cham, IL, 2015, pp. 203–221.